Journal of Sound and Vibration (2000) **229**(5), 1193–1212
doi:10.1006/jsvi.1999.2593, available online at http://www.idealibrary.com on IDEAL®

SOME OBSERVATIONS OF MODELLING OF WAVE MOTION IN LAYER-BASED ELASTIC MEDIA

R. ZHANG

Division of Engineering, Colorado School of Mines, Golden, CO 80401, *U.S.A.*

(*Received* 18 *September* 1998, *and in final form* 16 *August* 1999)

This paper aims to provide some observations on the merits and disadvantages of Cartesian and cylindrical co-ordinate representations (CaCR and CyCR) in modelling of wave propagation in layer-based elastic media and its engineering applications. The observations focus on (1) difference and consistency in solution procedure for wave motion in layer-based elastic media, (2) identification of its fundamental properties, (3) computational efficiency in relation to wave motion synthetics/simulation, and (4) basis for the applications to stochastic wave motion modelling associated with uncertainty in complex medium structure as well as source mechanism. Specifically, modelling of earthquake wave motion in a layer-based elastic half-space is used for illustration. As a foundation for the investigation, CaCR and CyCR for three-dimensional (3-D) wave motion are first constructed in a concise and consistent form. Consequently, some basic characteristics of 3-D wave motion in layered media (e.g., various surface waves) can then be identified in a unified form for the aforementioned different co-ordinate representations. More importantly, the succinct representations for 3-D wave motion provide a stepping stone for further study on wave motion modelling with uncertainty in the Earth medium and source mechanism. These and the other pertinent issues will be investigated in this study from the viewpoint of systematic computer code development and computational efficiency, which is substantial to practical engineering applications.

1. INTRODUCTION

Among continuum mechanics models for wave motions in layer-based elastic media, Cartesian and cylindrical co-ordinate representations (CaCR and CyCR) are probably the most widely used approaches as far as their engineering applications are concerned (see Figure 1). While both approaches are well-established theoretically in the past decades, further studies are needed with respect to their engineering applications from the viewpoint of systematic computer code development and computational efficiency, due to the rapid advances of computer technology.

Mathematically, 3-D wave motion in an elastic and homogeneous half-space can be effectively solved by applying an integral transform approach. The pertinent first study could historically date back to 1904 to Lame's problem [1]. Although a large number of references in this area can be found in monographs [2–5], some recent

0022-460X/00/051193 + 20 $35.00/0

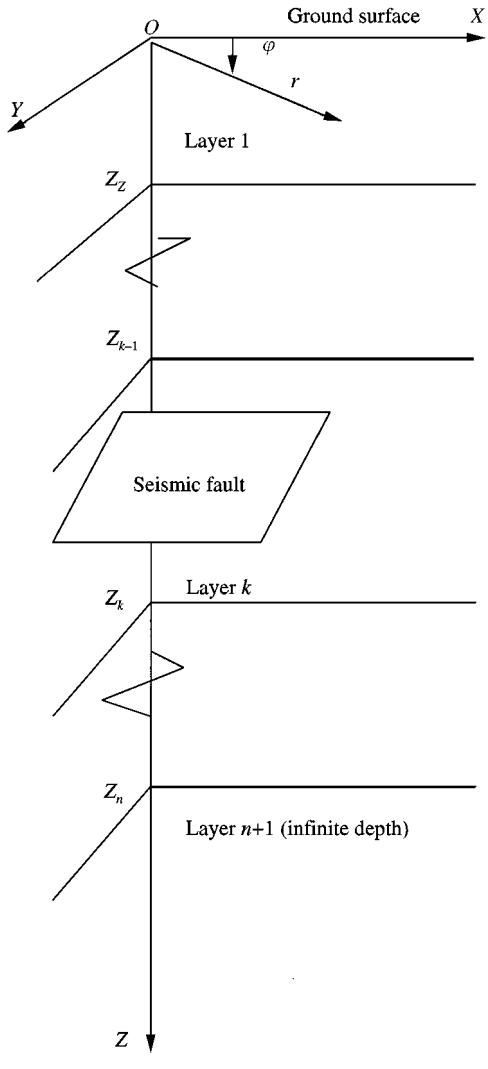

Figure 1. CaCR and CyCR for a layered half-space with a seismic source.

developments, especially those associated with the applications of advanced computer technology into structural and geotechnical earthquake engineering, have been made in the last two decades. In particular, the CaCR for wave motion is further developed in references [6–12], etc., while the CyCR is in detail analyzed in references [13–20], among others. While significant improvements have been made in computational efficiency and accuracy in 3-D wave motion modelling with the use of either CaCR or CyCR, little attention has been paid to (1) difference and consistency in the solution procedure for wave motion, (2) consistency in identifying its fundamental properties, (3) computational efficiency in relation to wave motion synthetics/simulation, and (4) basis for further applications to stochastic wave motion modelling associated with uncertainty in the complex medium structure as well as the source mechanism.

One of the purposes of this study is to integrate previous theoretical investigations and thus to provide an analysis of 3-D wave motion in a general and unified form. For illustration, modelling of earthquake wave motion in a layered half-space is used. Specifically, CaCR and CyCR for 3-D wave motion are constructed in a concise and consistent form. Consequently, some fundamental characteristics of 3-D wave motion in layered media (e.g., various surface waves) can then be identified in a compatible form for the aforementioned different co-ordinate representations. More importantly, the concise representations for 3-D wave motion provide a stepping stone for further study on wave motion with uncertainty in earth medium and seismic sources. These and the other pertinent issues will be finally examined from the viewpoint of systematic computer code development and computational efficiency, which is substantial to practical engineering applications.

2. CaCR AND CyCR FOR WAVE MOTIONS

2.1. PROBLEM STATEMENT

Earthquake wave motion is the result of propagating seismic waves in the Earth, which are originally generated by a seismic source. Therefore, appropriate modelling for wave motion in the Earth becomes crucially important for synthesizing realistic earthquake wave motion.

Based on previous studies, seismic source mechanism can usually be described as a slip or dislocation rupturing over a certain area of a fault, while the Earth is often modelled as vertically non-homogeneous media, idealized as a layered half-space with each layer being elastic and homogeneous (irregular surface/interfaces and heterogeneity will be discussed later). Within this framework, seismic waves can then be obtained by solving governing equations of motion subjected to a series of double-couple forces that are equivalent to dislocations in the broken fault area. In doing so, it is also required to have pertinent conditions satisfied that are the continuity conditions at each layer-to-layer interface and boundary conditions at both free ground surface and infinite (radiation condition).

2.2. FINITE INTEGRAL TRANSFORMATION APPROACH

For the sake of computational efficiency, the aforementioned problem is usually solved in the frequency–wave number domain, instead of the time–space domain, with the aid of finite integral transformation approaches. Specifically, triple-finite Fourier transforms are applied in CaCR for each and every physical quantity involved (e.g., components of displacements and stresses) between the time–space domain (x, y, t) and the frequency–wave number domain $(\kappa_x, \kappa_y, \omega)$, while double-finite Fourier transforms and a finite Hankel transform are used in CyCR between the time–space domain (r, θ, t) and the frequency–azimuthal order–wave number domain (κ_r, n, ω). It is noted that n represents azimuthal order, and $(\kappa_x, \kappa_y, \kappa_r)$ denote wave numbers in x, y and r directions, respectively, with $\kappa_r^2 = \kappa_x^2 + \kappa_y^2$. The wave motion responses in the transformed domain can then be

found by solving a set of ordinary differential equations in each layer with depth index z as the only variable. Such an approach will facilitate the solution procedure not only for wave propagation in layers as well as wave reflection and refraction at interfaces and boundaries, but also for the waves generated by a seismic dislocation source. After the wave motion responses in transformed domain are obtained, the associated responses in the time–space domain can then be found by performing the corresponding triple-inverse transformation.

To this end, wave motion representations become essential to the problem at hand.

2.3. REPRESENTATIONS FOR WAVE MOTIONS

By integrating previous pertinent studies, it can be shown that displacements and stresses in time–space domain can be represented by a concise and consistent form with the aid of orthogonal vector harmonics in transformed domain:

$$\mathbf{u}(\alpha, \beta, z, t) = C_\chi \sum_l \sum_m \sum_n \mathrm{e}^{\mathrm{i}\omega t}(W_R \mathbf{e}_R + W_S \mathbf{e}_S + W_T \mathbf{e}_T), \tag{1}$$

$$\mathbf{t}(\alpha, \beta, z, t) = C_\chi \sum_l \sum_m \sum_n \omega \mathrm{e}^{\mathrm{i}\omega t}(F_R \mathbf{e}_R + F_S \mathbf{e}_S + F_T \mathbf{e}_T), \tag{2}$$

where $\mathbf{u}(\alpha, \beta, z, t) = u_\alpha \mathbf{e}_\alpha + u_\beta \mathbf{e}_\beta + u_z \mathbf{e}_z$ and $\mathbf{t}(\alpha, \beta, z, t) = \sigma_{\alpha z} \mathbf{e}_\alpha + \sigma_{\beta z} \mathbf{e}_\beta + \sigma_{zz} \mathbf{e}_z$ are, respectively, vectors of displacements and stresses in the time–space domain, while $(\mathbf{e}_R, \mathbf{e}_S, \mathbf{e}_T)$ and (W_ξ, F_ξ, C_χ), $\xi = R$, S or T, $\chi = a$ or y, denote orthogonal vector harmonics and corresponding coefficients. It is noted that $(\mathbf{e}_\alpha, \mathbf{e}_\beta, \mathbf{e}_z)$ are orthogonal unit vectors in α, β, and z directions, where the pair (α, β) denotes (x, y) for CaCR and (r, θ) for CyCR. It can be shown (e.g., references [12, 15]) that (W_ξ, F_ξ) are related to the magnitudes of coupled P-SV wave motion if $\xi = R$ and/or S, and to the magnitudes of SH wave motion if $\xi = T$.

Equations (1) and (2) indicate that three orthogonal components of physical quantities in the time–space domain are decomposed into a series (triple summations) of orthogonal components in the transformed domain, each of which is associated with P-SV or SH wave motion component.

For CaCR, $C_\chi = C_a \equiv \pi^3/(T_W X_W Y_W)$ represents a co-ordinate-system-based coefficient with (X_W, Y_W, T_W) being half-window lengths in the time–space domain. The window size is selected so that the synthesized or simulated wave motion within the window will not have alias signals due to window repetition. The explicit expression for $(\mathbf{e}_R, \mathbf{e}_S, \mathbf{e}_T)$ in CaCR is

$$\mathbf{e}_R = \exp(\mathrm{i}\kappa_x x + \mathrm{i}\kappa_y y)\mathbf{e}_z, \tag{3}$$

$$\mathbf{e}_S = \left(\frac{\mathrm{i}\kappa_x}{\kappa_r}\mathbf{e}_x + \frac{\mathrm{i}\kappa_y}{\kappa_r}\mathbf{e}_y\right)\exp(\mathrm{i}\kappa_x x + \mathrm{i}\kappa_y y), \tag{4}$$

$$\mathbf{e}_T = \left(\frac{\mathrm{i}\kappa_y}{\kappa_r}\mathbf{e}_x - \frac{\mathrm{i}\kappa_x}{\kappa_r}\mathbf{e}_y\right)\exp(\mathrm{i}\kappa_x x + \mathrm{i}\kappa_y y), \tag{5}$$

where $\kappa_x = m\pi/X_W$, $\kappa_y = n\pi/Y_W$ and $\omega = l\pi/T_W$ with m, n and l being integers. Conversely, the variables W_ξ and F_ξ can be found in terms of displacements and stresses in time–space domain:

$$W_\xi(\kappa_x, \kappa_y, z, \omega) = \frac{1}{(2\pi)^3} \int_{-T_W}^{T_W} e^{-i\omega t}\, dt \int_{-X_W}^{X_W} dx \int_{-Y_W}^{Y_W} dy \{\mathbf{u} \cdot \mathbf{e}_\xi^*\}, \tag{6}$$

$$F_\xi(\kappa_x, \kappa_y, z, \omega) = \frac{1}{\omega(2\pi)^3} \int_{-T_W}^{T_W} e^{-i\omega t}\, dt \int_{-X_W}^{X_W} dx \int_{-Y_W}^{Y_W} dy \{\mathbf{t} \cdot \mathbf{e}_\xi^*\}, \tag{7}$$

where the asterisk denotes a complex conjugate and the dot between two vectors stands for dot or inner product.

For CyCR, $C_\chi = C_y \equiv 2\pi/T_W/[R_W J_n'(\kappa_r R_W)]^2$ with R_W being the truncated length in radial direction, J_n the nth order Bessel function of the first kind, and the prime on J the first derivative of J with respect to its argument. The explicit expression for $(\mathbf{e}_R, \mathbf{e}_S, \mathbf{e}_T)$ in CyCR is

$$\mathbf{e}_R = J_n(\kappa_r r) \exp(in\varphi)\mathbf{e}_z, \tag{8}$$

$$\mathbf{e}_S = [J_n'(\kappa_r r)\mathbf{e}_r + \frac{in}{\kappa_r r} J_n(\kappa_r r)\mathbf{e}_\varphi] \exp(in\varphi), \tag{9}$$

$$\mathbf{e}_T = \left[\frac{in}{\kappa_r r} J_n(\kappa_r r)\mathbf{e}_r - J_n'(\kappa_r r)\mathbf{e}_\varphi\right] \exp(in\varphi), \tag{10}$$

where κ_r are the roots of the transcendental equations of $J_n(\kappa_r R_W) = 0$. Similarly, variables W_ξ and F_ξ can be found as

$$W_\xi(\kappa_r, n, z, \omega) = \frac{1}{(2\pi)^2} \int_{-T_W}^{T_W} e^{-i\omega t}\, dt \int_0^{R_W} r\, dr \int_0^{2\pi} d\varphi \{\mathbf{u} \cdot \mathbf{e}_\xi^*\}, \tag{11}$$

$$F_\xi(\kappa_r, n, z, \omega) = \frac{1}{\omega(2\pi)^2} \int_{-T_W}^{T_W} e^{-i\omega t}\, dt \int_0^{R_W} r\, dr \int_0^{2\pi} d\varphi \{\mathbf{t} \cdot \mathbf{e}_\xi^*\}. \tag{12}$$

2.4. CONSISTENCY IN TRANSFORMED DOMAIN

It can be shown that, with the use of wave representations of equations (1) and (2), the governing equations of wave motion in the transformed domain (without existence of external forces) are

$$\frac{d}{dz}\begin{Bmatrix} w \\ f \end{Bmatrix} = [A]\begin{Bmatrix} w \\ f \end{Bmatrix}, \tag{13}$$

where for P-SV waves, $[A]$ is a 4×4 matrix and its elements can be found as a function of layer properties, $w=\{W_R, W_S\}^{\mathrm{T}}$, and $f=\{F_R, F_S\}^{\mathrm{T}}$, while for SH waves, $[A]$ is a 2×2 matrix, $w=W_T$, and $f=F_T$. Based on the physical meanings of (W, F), the coefficient pair (w, f) is thus related to either P-SV or SH wave motion.

As indicated in section 2.1, a seismic source mechanism can be described as a dislocation rupturing over a fault. If the size of a broken fault area is comparable to the dominant seismic wavelength and/or the distance to an observation site, which is usually so for nearfield motion, dislocation at the fault area can be replaced by a series of double-couple forces, each of which is proportional to the discretized sub-fault area, its associated final dislocation amplitude as well as surrounding rigidity. It can be shown that with the use of continuity conditions at each layer-to-layer interface and boundary conditions at both surface and infinite, wave responses at depth z in the transformed domain subjected to the dislocation at the jth sub-fault, i.e., coefficients (W_ξ, F_ξ) or (w, f) at given $(\kappa_x, \kappa_y, z, \omega)$ or (κ_r, n, z, ω), can then be found as follows:

$$\begin{Bmatrix} w \\ f \end{Bmatrix} = \begin{bmatrix} M_u(i) & M_d(i) \\ N_u(i) & N_d(i) \end{bmatrix} \begin{Bmatrix} I \\ R(z,0) \end{Bmatrix} [I - R(z, z_{sj}^-)R(z,0)]^{-1} T(z_{sj}^-, z)$$

$$[I - R(z_{sj}^+, \infty)R(z_{sj}^-, 0)]^{-1} \mathrm{i}\{[N_d^{\mathrm{T}}(k) + R(z_{sj}^+, \infty)N_u^{\mathrm{T}}(k)]\Delta w_{sj}$$

$$- [M_d^{\mathrm{T}}(k) + R(z_{sj}^+, \infty)M_u^{\mathrm{T}}(k)]\Delta f_{sj}\} \tag{14}$$

if $z_{i-1}^+ < z < z_i^- < z_s$, and

$$\begin{Bmatrix} w \\ f \end{Bmatrix} = \begin{bmatrix} M_u(i) & M_d(i) \\ N_u(i) & N_d(i) \end{bmatrix} \begin{Bmatrix} R(z, \infty) \\ I \end{Bmatrix} [I - R(z_{sj}^+, z)R(z, \infty)]^{-1} T(z_{sj}^+, z)$$

$$[I - R(z_{sj}^+, \infty)R(z_{sj}^-, 0)]^{-1} \mathrm{i}\{[R(z_{sj}^-, 0)N_d^{\mathrm{T}}(k) + N_u^{\mathrm{T}}(k)]\Delta w_{sj}$$

$$- [R(z_{sj}^-, 0]M_d^{\mathrm{T}}(k) + M_u^{\mathrm{T}}(k)]\Delta f_{sj}\} \tag{15}$$

if $z_{i-1}^+ > z > z_i^- > z_s$. In the above equations, coefficient i denotes imaginary unit $\sqrt{-1}$ while i in the subscripts and parentheses stands for layer number. Therefore, z_{i-1} indicates the depth of the ith interface ($i=1$ for surface), its superscript of $+$ or $-$ corresponds to the lower or upper side of the interface, z_{sj} is the depth of the dislocation at the jth sub-fault (Δw_{sj}, Δf_{sj}) are the discontinuities of (w, f) in the jth sub-source area which are equivalent to the effects of a seismic dislocation sources at z_s and can be found in references [12, 15]. In addition, columns in a matrix with sub-matrices $M(i)$ and $N(i)$ are the eigenvectors of matrix $[A]$ in layer i, $R(z_i, z_j)$ and $T(z_i, z_j)$ are known as reflection and transmission matrices, respectively, which characterize properties of wave propagation in the earth medium between depths z_i and z_j. The explicit expressions of all the aforementioned matrices can be found in Appendix A.

At this junction, it is of interest to note that the response form in the transformed domain, i.e. equations (14) and (15), is the same for both CaCR and CyCR.

The corresponding wave responses in time–space domain can finally be found by using equations (1) and (2) or the explicit form

$$\mathbf{u}(\alpha, \beta, z, t) = \sum_j \mathbf{u}(\alpha, \beta, z, t; \alpha_{sj}, \beta_{sj}, z_{sj}, t_{sj}), \tag{16}$$

$$\mathbf{t}(\alpha, \beta, z, t) = \sum_j \mathbf{t}(\alpha, \beta, z, t; \alpha_{sj}, \beta_{sj}, z_{sj}, t_{sj}), \tag{17}$$

where

$$\mathbf{u}(\alpha, \beta, z, t; \alpha_{sj}, \beta_{sj}, z_{sj}, t_{sj}), = C_\chi \sum_l \sum_m \sum_n \mathrm{e}^{\mathrm{i}\omega t}(\tilde{u}_\alpha \mathbf{e}_\alpha + \tilde{u}_\beta \mathbf{e}_\beta + \tilde{u}_z \mathbf{e}_z), \tag{18}$$

$$\mathbf{t}(\alpha, \beta, z, t; \alpha_{sj}, \beta_{sj}, z_{sj}, t_{sj}), = C_\chi \sum_l \sum_m \sum_n \omega \mathrm{e}^{\mathrm{i}\omega t}(\tilde{\sigma}_{\alpha z} \mathbf{e}_\alpha + \tilde{\sigma}_{\beta z} \mathbf{e}_\beta + \tilde{\sigma}_{zz} \mathbf{e}_z), \tag{19}$$

are the responses due to jth point source at $(\alpha_{sj}, \beta_{sj}, z_{sj}, t_{sj})$, in which $\tilde{u}$ and $\tilde{\sigma}$ are the components of displacements and stresses in transformed domain, which can be easily found in terms of (W_ξ, F_ξ) from equations (1)–(5) and (8)–(10). In particular, $\tilde{u}$ can be represented in CaCR by

$$\tilde{u}_x = \left(\frac{\mathrm{i}\kappa_x}{\kappa_r} W_S + \frac{\mathrm{i}\kappa_y}{\kappa_r} W_T\right) \exp(\mathrm{i}\kappa_x x + \mathrm{i}\kappa_y y), \tag{20}$$

$$\tilde{u}_y = \left(\frac{\mathrm{i}\kappa_y}{\kappa_r} W_S - \frac{\mathrm{i}\kappa_x}{\kappa_r} W_T\right) \exp(\mathrm{i}\kappa_x x + \mathrm{i}\kappa_y y), \tag{21}$$

$$\tilde{u}_z = W_R \exp(\mathrm{i}\kappa_x x + \mathrm{i}\kappa_y y) \tag{22}$$

and in CyCR by

$$\tilde{u}_r = [\mathrm{J}_n'(\kappa_r r) W_S + \frac{\mathrm{i}n}{\kappa_r r} \mathrm{J}_n(\kappa_r r) W_T] \exp(\mathrm{i}n\varphi), \tag{23}$$

$$\tilde{u}_\varphi = \left[\frac{\mathrm{i}n}{\kappa_r r} \mathrm{J}_n(\kappa_r r) W_S - \mathrm{J}_n'(\kappa_r r) W_T\right] \exp(\mathrm{i}n\varphi), \tag{24}$$

$$\tilde{u}_z = \mathrm{J}_n(\kappa_r r) W_R \exp(\mathrm{i}n\varphi). \tag{25}$$

3. FUNDAMENTAL RESPONSE PROPERTIES

As seen from equations (14) and (15), the responses will become infinite or singular at a certain set of $(\kappa_x, \kappa_y, \omega)$ or (κ_r, n, ω) if damping of the media is not

considered. Such singularities can be identified and related to special travelling waves in the Earth, in the forms of P and S waves in a layer medium and surface waves near ground surface or interfaces. This is detailed as follows, attempting to provide a unified version without referring to a specific co-ordinate system involved.

3.1. HORIZONTALLY PROPAGATING P AND S WAVES

The singularities in matrices $M(i)$ and $N(i)$ of equations (14) and (15) can be found if $\varepsilon_{Pi} = \infty$ and/or $\varepsilon_{Si} = \infty$. This is equivalent to (see equations (A1)–(A5))

$$q_{Pi} = (\sqrt{1/v_{Pi}^2 - \kappa_r^2/\omega^2} = 0, \qquad q_{Si} = (\sqrt{1/v_{Si}^2 - \kappa_r^2/\omega^2} = 0 \tag{26}$$

which results in wavenumbers $\kappa_r(P)$ and $\kappa_r(S)$ for P and S waves as

$$\kappa_r(P) = \omega/v_{Pi}, \qquad \kappa_r(S) = \omega/v_{Si}. \tag{27}$$

Since ωq_{Pi} and ωq_{Si} represent the wavenumbers in the z direction for P and S waves, respectively (see equation (A8)), equation (26) or (27) implies that waves with the wave numbers in layer i being $\kappa_r(P)$ and $\kappa_r(S)$ are the horizontally propagating P and S waves. Since such waves never propagate away from the depth at which they are, it is obvious that those waves will not contribute to the responses of equations (14) and (15).

3.2. RAYLEIGH WAVES

As a special case, consider a P-SV wave motion in a uniform half-space. The singularities can then be found by letting the denominator of response expression in equations (14) and (15) be zero (e.g., the denominator of $R(z, 0)$ equals zero in equation (14)), or equivalently $|N_d(1)| = 0$ (see equation (A15)). This yields, with the aid of equation (A2)

$$|N_d(1) = \begin{vmatrix} \rho_1(2v_{S1}^2\kappa_r^2/\omega^2 - 1)\varepsilon_{P1} & 2\mathrm{i}\rho_1 v_{S1}^2 \kappa_r q_{S1}\varepsilon_{S1}/\omega \\ 2\mathrm{i}\rho_1 v_{S1}\kappa_r q_{P1}\varepsilon_{P1}/\omega & \rho_1(2v_{S1}^2\kappa_r^2/\omega^2 - 1)\varepsilon_{S1} \end{vmatrix} = 0 \tag{28a}$$

or

$$[2\kappa_r^2/\omega^2 - 1/v_{S1}^2]^2 - 4\kappa_r^2 q_{P1} q_{S1}/\omega^2 = 0 \tag{28b}$$

which is the well-known equation for Rayleigh wave in a half-space. It can be shown (e.g., reference [2]) that $\kappa_r(R)$, root of equation (28b), will be greater than $\kappa_r(S)$. For a layered half-space, the denominator of equations (14) and (15) is very complicated. Its zeros cannot, therefore, be expressed in simple closed forms.

3.3. STONELEY WAVES

Stoneley waves are a special form of a coupled P-SV wave motion, occurring at the interface of two neighboring but different-property solid media. It propagates along the interface and decays exponentially with the distance away from the interface. Because of the aforementioned properties, the singularity associated with Stoneley waves can then be found by examining singularities of wave responses at the interface, which are related to the wave reflection and transmission at the interface (see equations (A9)–(A14)). It can be found that the singularities of wave reflection and transmission (R and T) across the interface happen at the condition (see equations (A9) and (A10))

$$Q_{22} = \mathrm{i}N_u^{\mathrm{T}}(i)M_d(i+1) - \mathrm{i}M_u^{\mathrm{T}}(i)N_d(i+1) = 0. \tag{29}$$

With the aid of equations (A1) and (A2), equation (29) is reduced to

$$c_6(\kappa_r/\omega)^6 + c_4(\kappa_r/\omega)^4 + c_2(\kappa_r/\omega)^2 + c_0 = 0, \tag{30}$$

where

$$c_6 = 4v_{Si}^4 v_{S(i+1)}^4(\mu_i - \mu_{i+1})^2, \tag{31}$$

$$c_4 = 4v_{Si}^4 v_{S(i+1)}^4(q_{Pi}q_{Si} - q_{P(i+1)}q_{S(i+1)})(\mu_i - \mu_{i+1})^2 + 4v_{Si}^2 v_{S(i+1)}^2(\mu_i\mu_{i+1}v_{Si}^2 + \mu_i\mu_{i+1}v_{S(i+1)}^2 - \mu_i^2 v_{S(i+1)}^2 - \mu_{(i+1)}^2 v_{Si}^2), \tag{32}$$

$$c_2 = 4v_{Si}^4 v_{S(i+1)}^4 q_{Pi}q_{Si}q_{P(i+1)}q_{S(i+1)}(\mu_i - \mu_{i+1})^2 + 4v_{Si}^2 v_{S(i+1)}^2(\mu_i\mu_{i+1}v_{Si}^2 q_{Pi}q_{Si} + \mu_i\mu_{i+1}v_{S(i+1)}^2 q_{P(i+1)}q_{S(i+1)} - \mu_i^2 v_{S(i+1)}^2 q_{P(i+1)}q_{S(i+1)} - \mu_{(i+1)}^2 v_{Si}^2 q_{Pi}q_{Si}) + (\mu_i v_{S(i+1)}^2 - \mu_{i+1}v_{Si}^2)^2, \tag{33}$$

$$c_0 = \mu_i^2 v_{S(i+1)}^4 q_{P(i+1)}q_{S(i+1)} + \mu_i\mu_{(i+1)}v_{Si}^2 v_{S(i+1)}^2 q_{Pi}q_{S(i+1)} + \mu_i\mu_{i+1}v_{Si}^2 v_{S(i+1)}^2 q_{P(i+1)}q_{Si} + \mu_{(i+1)}^2 v_{Si}^4 q_{Pi}q_{Si}, \tag{34}$$

in which $\mu_i = \rho v_{Si}^2$. It can be shown that equation (30) is completely consistent with equation (5.110) in reference [2], despite the different approaches used in obtaining them.

3.4. LOVE WAVES

Love waves are a special form of SH wave motion, occurring only in a layered half-space. It can be verified easily that no singularity exists in equations (14) and (15) for an SH wave motion in a uniform half-space. For the two-layer half-space, the singularities can be identified by letting the denominator of the SH wave

responses in equations (14) and (15) be zero. This leads to

$$\rho_1 v_{S1}^2 q_{S1} + \rho_2 v_{S2}^2 q_{S2} = \exp(2\mathrm{i}\omega q_{S1} z_1)(\rho_1 v_{S1}^2 q_{S1} - \rho_2 v_{S2}^2 q_{S2}), \tag{35}$$

which could be simplified as

$$\tan(\omega q_{S1} z_1) = \mathrm{i}\rho_2 v_{S2}^2 q_{S2}/(\rho_1 v_{S1}^2 q_{S1}). \tag{36}$$

The above equation is the well-known equation for Love waves in a two-layer half-space. It can also be shown that $\kappa_r(L)$, the solution of equation (36), is between $\kappa_r(S_1)$ and $\kappa_r(S_2)$. The singularities associated with *SH* waves in a half-space consisting of more than two layers cannot be expressed in a simple form.

4. COMPUTATIONAL EFFICIENCY

While both CaCR and CyCR can theoretically be used to obtain wave responses, computational efficiency is probably one of the most common concerns for its practical engineering applications. At this junction, computational issues for wave motion responses in the following three aspects are examined, in order to provide some observations on computational efficiency of these two representations.

4.1. SINGLE OBSERVATION SITE WITH A POINT SOURCE

Since wave responses in the transformed domain to a point source (e.g., (W, F) or (w, f) or $(\tilde{u}, \tilde{\sigma})$) can be obtained at almost the same computational effort for both CaCR and CyCR, the difference in computational time for these two approaches is thus the triple-inverse transformation or summation (equations (18) and (19)). This difference can be further narrowed down to double summations of m and n, since summation on l is the same, which is related to the time–frequency transformation. For a given-size window, say $R_W = \sqrt{X_W^2 + Y_W^2}$, the summation effort on m (or n) for κ_x (or κ_y) in CaCR will be almost the same as for κ_r in CyCR, in order to achieve the same resolution. Therefore, computational efficiency of these two approaches can be simply perceived from the computational effort on the summation of n, which is related to κ_y in CaCR and to azimuthal order in CyCR. It can be shown [15] that the azimuthal order will be in the range of $[-2, 2]$ for any kind of dislocation source, leading the summation of n in CyCR to five terms at maximum. In contrast, even if some quadruple symmetric or antisymmetric properties are used in CaCR, which will reduce the summation effort on n to approximately one-sixteenth at most while keeping the same resolution as m, the total summation effort on n in CaCR, related to κ_y, will still be much greater than its counterpart in CyCR, in order to obtain its reasonable resolution.

To this end, it is obvious that CyCR is computationally much more efficient in obtaining the responses at single observation site to a point source, i.e. equations (18) and (19), than CaCR.

4.2. SINGLE OBSERVATION SITE WITH MULTIPLE POINT SOURCES

In view of the above facts, the computational effort will be different for CaCR and CyCR to obtain the responses to multiple point sources, depending strongly on the number of point sources as well as the location of observations.

Since the Fourier transformation has the shift property

$$\mathscr{T}\{f(x-x_s, y-y_s)\} = \mathrm{e}^{\pm(\mathrm{i}\kappa_x x_s + \mathrm{i}\kappa_x y_s)}\mathscr{T}\{f(x, y)\}, \tag{37}$$

where $\mathscr{T}$ denotes Fourier transformation (either forward or backward), the summation on j (number of point sources) can be exchanged with the summation on l, m and n in equations (16)–(19). As an example, the wave responses of equation (16) in CaCR can be rewritten with the aid of equations (14), (15) and (18) as

$$\mathbf{u}(\mathbf{x}, \mathbf{y}, \mathbf{z}, \mathbf{t}) = \mathbf{C}_a \sum_l \sum_m \sum_n \mathrm{e}^{\mathrm{i}\omega t}\left[\sum_j (\tilde{u}_x \mathbf{e}_x + \tilde{u}_y \mathbf{e}_y + \tilde{u}_z \mathbf{e}_z)\right], \tag{38}$$

where $\sum_j \tilde{u}$ can be found in terms of $\sum_j W$ shown in equations (20)–(22) or more specifically $\sum_j w$ (note: the relationship between (w, f) and (W, F) can be seen in the paragraph after equation (13)) from the following equation with the aid of equations (14) and (15):

$$\begin{Bmatrix} \sum_j w \\ \sum_i f \end{Bmatrix} = \begin{bmatrix} M_u(i) & M_d(i) \\ N_u(i) & N_d(i) \end{bmatrix} \begin{Bmatrix} I \\ R(z,0) \end{Bmatrix} \sum_j \langle [I - R(z, z_{sj}^-)R(z,0)]^{-1} T(z_{sj}^-, z)$$

$$[I - R(z_{sj}^+, \infty)R(z_{sj}^-, 0)]^{-1}\,\mathrm{i}\exp(\mathrm{i}\kappa_x x_{sj} + \mathrm{i}\kappa_y y_{sj})$$

$$\{[N_d^{\mathrm{T}}(k) + R(z_{sj}^+, \infty)N_u^{\mathrm{T}}(k)]\Delta w_{sj} - [M_d^{\mathrm{T}}(k) + R(z_{sj}^+, \infty)M_u^{\mathrm{T}}(k)]\Delta f_{sj}\}\rangle. \tag{39}$$

With the use of the composite rule of equations (A16) and (A17), the factors within summation on j in the above equation can usually be further reduced, thus greatly reducing the computational effort on summation of j. Its limited case is when all the point sources are located at the same depth, which leads equation (39) to

$$\begin{Bmatrix} \sum_j w \\ \sum_j f \end{Bmatrix} = \begin{bmatrix} M_u(i) & M_d(i) \\ N_u(i) & N_d(i) \end{bmatrix} \begin{Bmatrix} I \\ R(z,0) \end{Bmatrix} [I - R(z, z_s^-)R(z,0)]^{-1} T(z_s^-, z)$$

$$[I - R(z_s^+, \infty)R(z_s^-, 0)]^{-1}\,\mathrm{i}\sum_j \langle \exp(\mathrm{i}\kappa_x x_{sj} + \mathrm{i}\kappa_y y_{sj})$$

$$\{[N_d^{\mathrm{T}}(k) + R(z_s^+, \infty)N_u^{\mathrm{T}}(k)]\Delta w_{sj} - [M_d^{\mathrm{T}}(k) + R(z_s^+, \infty)M_u^{\mathrm{T}}(k)]\Delta f_{sj}\}\rangle. \tag{40}$$

Equation (38) in conjunction with equation (39) or (40) indicates that the computational time for wave responses at given single observation sites to multiple point sources will be much less than the time needed for a point source multiplying by the number of point sources. In other words, the computational effort for multiple point sources is slightly more than that for a point source in CaCR.

In contrast, CyCR does not have such summation exchange advantages as CaCR, since the Hankel transformation in CyCR does not have similar simple shift properties as the Fourier transformation in CaCR. Therefore, the computational effort for wave responses to multiple point sources in CyCR will be simply the multiple times of the effort for wave responses to a point source, although the former will be usually less than the latter in practical computation since most of the coefficients need to be calculated only once with respect to the summation on j.

With the above in mind, it could then be concluded that CaCR will be more computationally efficient than CyCR if the number of point sources is relatively large. Otherwise, CyCR is better in terms of computational efficiency. For illustration, an example is given as follows as a very rough estimation. If the number of point sources is equal to or larger than $n/(5 \times 16)$, then CaCR is computationally efficient. In this calculation, it is assumed that the summation on n in CyCR has five terms (which is also at maximum) and the summation on n in CaCR is reduced to $n/16$ due to full utilization of quadruple symmetry (it will not be achieved in practice). Otherwise, CyCR is better.

4.3. NEAR-FIELD MOTION AT DENSE OBSERVATION SITES

As one of the most important engineering applications of seismic wave motion modelling, nearfield ground motion at dense observation sites is needed. The pertinent purposes are multiple, e.g., in examining such nature of ground motion as spatial variations and developing a seismic intensity map, etc. In addition, due to lack of sufficient seismometers at the nearfield ground surface, synthesis or simulation of nearfield motion at dense observations becomes substantial, particularly after the 1994 Northridge and the 1995 Kobe earthquakes.

It is for the nearfield motion under consideration that the detailed information of the source mechanism becomes much more important than for farfield motion. Accordingly, fine discretization of a seismic fault is usually required. This is equivalent to a large summation on j in equations (16) and (17). In the light of comments on computational efficiency discussed in section 4.2, CaCR is thus computationally more efficient than CyCR in the situation at hand. In addition, since nearfield motions at dense observation sites are needed, the two-fold summation on m and n in CaCR can be carried out by FFT, which will significantly increase the computational efficiency by using CaCR to solve the problem at hand compared with CyCR.

The observations from this section have also been verified in the past decade with the use of two computer codes entitled "SEISMO" and "STOQUK", which are described in Appendix B.

5. FURTHER APPLICATIONS

While equations (16) and (17) could be used to synthesize or simulate seismic wave motions in a layered half-space generated by an extended source, uncertainty in both seismic source and Earth media has not been considered in the aforementioned models, which will make the problem at hand more complicated. The latter is particularly important to the nature of nearfield motion and its implication for damage of large-scale structural and geotechnical engineering systems. Nevertheless, the aforementioned model can be used as a stepping stone to construct a more realistic seismic wave motion model by taking into consideration various uncertainties.

5.1. IRREGULARITY AND HETEROGENEITY

As an example, consider the Earth as a layered half-space with slightly irregular boundaries (surface or layer-to-layer interfaces) and/or laterally heterogeneous layer properties. Seismic waves are originally generated by an extended seismic dislocation source buried in one of the layers, say layer k, and then propagating through the Earth media. They can be obtained by solving the governing equation

$$\ell\{\mathbf{u}(\alpha, \beta, z, t)\} = \mathbf{p}(\alpha, \beta, z, t) \tag{41}$$

in conjunction with pertinent continuity and boundary conditions. In equation (41), ℓ is a linear operator, characterizing the layered half-space with lateral heterogeneity/irregularity and being a function of the layer properties (such as wave speeds and density in one layer) and the structure of the Earth media (such as depths of irregular interfaces); and $\mathbf{p} = p_x\mathbf{e}_x + p_y\mathbf{e}_y + p_z\mathbf{e}_z$ is the body force equivalent to the effect of the dislocation at the broken seismic fault. The profile of the irregular boundaries can be expressed by

$$z_j(\alpha, \beta) = z_j^m + \varepsilon z_j^s(\alpha, \beta), \tag{42}$$

where z_j is the depth of lower bound of layer j ($j = 1$ in Figure 1), superscript m denotes the corresponding mean part, and superscript s the corresponding perturbed part. Similarly, the properties of laterally heterogeneous layer j can be described by

$$\chi_j(\alpha, \beta) = \chi_j^m + \varepsilon\chi_j^s(\alpha, \beta), \tag{43}$$

where χ_j represents the P wave speed, S wave speed or density of layer j respectively. Correspondingly, the displacements may also be decomposed into two parts,

$$\mathbf{u}(\alpha, \beta, z, t) = \mathbf{u}^m(\alpha, \beta, z, t) + \varepsilon\mathbf{u}^s(\alpha, \beta, z, t), \tag{44}$$

where $\mathbf{u}^m$ is referred to as the mean wave field and $\varepsilon\mathbf{u}^s$ as the scattered wave field. Since the linear operator ℓ is a function of the laterally heterogeneous layer

properties and the depths of irregular boundaries, it may be expanded as a Taylor series with respect to the corresponding mean values as

$$\ell = \ell^m + \varepsilon \ell^s + O(\varepsilon^2), \tag{45}$$

where ℓ^m denotes the mean linear operator, characterizing the wave motion in a layered half-space without lateral heterogeneity/irregularity; $\varepsilon \ell^s$ stands for the first order scattered linear operation due to the lateral heterogeneity/irregularity; and $O(\varepsilon^2)$ denotes the order of ε^2 and higher terms which may be neglected in the study, since the first order perturbation approach is considered adequate to reveal the fundamental characteristics of the seismic waves in the layered half-space with slightly lateral heterogeneity/irregularity.

Substituting equations (44) and (45) into equation (41) and neglecting the second and higher order of smallness ε, the following two sets of equations instead of one (i.e. equation (41)) for the original problem can be found as

$$\ell^m\{\mathbf{u}^m(\alpha, \beta, z, t)\} = \mathbf{p}(\alpha, \beta, z, t), \qquad \ell^m\{\mathbf{u}^s(\alpha, \beta, z, t)\} = \mathbf{p}^s(\alpha, \beta, z, t), \tag{46, 47}$$

where for each irregular surface/interface and/or laterally heterogeneous layer,

$$\mathbf{p}^s(\alpha, \beta, z, t) = -\ell^s\{\mathbf{u}^m(\alpha, \beta, z, t)\} \quad \text{if } z = z_j^m \quad \text{and/or} \quad z_j \leqslant z \leqslant z_{j+1}. \tag{48}$$

The physical meanings of equations (46) and (47) are quite obvious and can be explained as follows. Both the mean and the scattered wave fields share the same linear operator ℓ^m, which indicates that they should be computed on the basis of the same layered half-space without the existence of lateral heterogeneity/irregularity. The mean wave field is obtained first from equation (46) with body force $\mathbf{p}$ distributed in the seismic fault area in the source layer, which is equivalent to the effect of the seismic dislocation. The scattered wave field can then be found from equation (48) in which the distributed fictitious forces $\mathbf{p}^s$ are computed in terms of the mean wave field and the quantities of the lateral heterogeneity/irregularity involved in the operator ℓ^s (see equation (45)). The total wave field in a layered half-space with lateral heterogeneity/irregularity can finally be obtained as a superposition of these two fields via equation (44). The solution of wave motions in a perfectly layered half-space generated by equivalent body forces as described in equations (46) and (47) can be easily found by equations (16)–(19).

5.2. COMPUTATIONAL DIFFICULTIES WITH CyCR

Theoretically, both CaCR and CyCR can be applied to solve equations (46) and (47) and irregularity/heterogeneity problem. Practically, CyCR is very difficult to be used due to an unaffordable computational effort.

As seen from equations (46) and (47), the fictitious forces for the scattered wave field $\mathbf{p}^s$ are obtained in terms of irregularity/heterogeneity and mean wave field. If CaCR is used, the aforementioned forces in the time–space domain can be easily

transformed into those in the frequency–wave number domain. It can be shown [12] that with the shift properties of the Fourier transformation of equation (37), the scattered wave response in the transformed domain in the media with the deviation part of irregularity/heterogeneity being in the form of $e^{i(\kappa'_x x + \kappa'_y y)}$ is proportional to the mean wave field response in the transformed domain at a shift wave number pair. In other words,

$$\begin{Bmatrix} w^s(\kappa_x, \kappa_y, z, \omega; \kappa'_x, \kappa'_y) \\ f^s(\kappa_x, \kappa_y, z, \omega; \kappa'_x, \kappa'_y) \end{Bmatrix} = \mathfrak{R}\left(\begin{Bmatrix} w^m(\kappa_x - \kappa'_x, \kappa_y - \kappa'_y, z, \omega) \\ f^m(\kappa_x - \kappa'_x, \kappa_y - \kappa'_y, z, \omega) \end{Bmatrix} \right), \tag{49}$$

where $\mathfrak{R}$ denotes a known function. Therefore, given the Fourier representation of an irregularity (or heterogeneity),

$$z_j^s(x, y) = \frac{\pi^2}{X_W Y_W} \sum_{m'} \sum_{n'} \tilde{z}(\kappa'_x, \kappa'_y) e^{i(\kappa'_x x + \kappa'_y y)}, \tag{50}$$

where $\kappa'_x = m'\pi/X_W$ and $\kappa'_y = n'\pi/Y_W$, the scattered wave response in the transformed domain will be obtained as

$$\begin{Bmatrix} w^s(\kappa_x, \kappa_y, z, \omega) \\ f^s(\kappa_x, \kappa_y, z, w) \end{Bmatrix} = \frac{\pi^2}{X_W Y_W} \sum_{m'} \sum_{n'} \tilde{z}(\kappa'_x, \kappa'_y) \mathfrak{R}\left(\begin{Bmatrix} w^m(\kappa_x - \kappa'_x, \kappa_y - \kappa'_y, z, \omega) \\ f^m(\kappa_x - \kappa'_x, \kappa_y - \kappa'_y, z, \omega) \end{Bmatrix} \right). \tag{51}$$

We digress to comment on the importance of equations (49)–(51). Unlike the huge computational effort for the mean wave responses, which is described in section 2 or more specifically in equations (14)–(19), equation (49) indicates that the scattered wave responses can be obtained in terms of the solution of the mean wave field with the appropriate wave number shift. The known function $\mathfrak{R}$ in equation (49) is actually a symbolic, relating only to some necessary product of known factors and the mean wave responses. Since any irregularity is composed of a series of simple sinusoidal variations (see equation (50)), equation (49) is thus regarded as a fundamental solution of the scattered wave response to a sinusoidal irregularity. The general solution is then given by equation (51), consisting of all the fundamental solutions to different fundamental sinusoidal irregularities. Apparently, for the irregularity with only several dominant wavelengths which is the most common case, the summation on m' and n' is very small compared with the summation on m and n in equations (18) and (19). For the detailed analysis, the reader is referred to reference [18].

In contrast, since the Hankel transform in CyCR does not have similar and simple shift properties as the Fourier transform in CaCR, CyCR will obviously lose the corresponding computational efficiency as CaCR behaves. In particular, the scattered wave responses in CyCR cannot be found in such a direct and simple relationship with mean wave responses in the transformed domain as equation (51) for CaCR. They can be obtained only by solving another almost independent wave problem with the governing equations of motions being equation (47), similar to solving the mean wave motion of equation (46).

In addition, since most of the aforementioned uncertainties such as irregularity can be easily described or simulated in Cartesian co-ordinates using the simulation technique such as the spectrum representation method [21, 22], engineering applications of CaCR for wave motions are expected to be more rigorous and robust than CyCR.

6. CONCLUDING REMARKS

While observations from this study reveal that CaCR are more robust than CyCR in many engineering applications from the viewpoint of computational efficiency, systematic investigation and engineering applications of wave motion modelling, it never implies that CyCR is useless in one way or the other. Whenever cylindrical problems are at hand such as pile or circular foundation–soil interaction in a layered half-space, CyCR will be the best tool to perform the pertinent investigation (e.g., references [23, 24]).

Although the observations on CaCR and CyCR for 3-D wave motion are presented in this study mainly from the viewpoint of earthquake engineering applications, they could also be applied to other pertinent wave issues such as crack problems in sandwich-type composite plates.

ACKNOWLEDGMENTS

The author would like to express his sincere gratitude to Professors Y. K. Lin and M. Shinozuka for their valuable advice and encouragement for this study carried out in the last decade. This work was supported by the National Science Foundation with Grant Nos. CMS 9612127 and 9896070 with Dr. S. C. Liu as a program director, by the U.S. Geological Survey with Award No. 98CRSA1077, by the Western Alliance to Expand Student Opportunities with Award No. F98UR013, and by two grants from the Colorado Advanced Software Institute that is sponsored in part by the Colorado Commission on Higher Education, an agency of the State of Colorado. The opinions, findings and conclusions expressed herein are those of the author and do not necessarily reflect the views of the sponsors.

REFERENCES

1. H. Lamb 1904 *Philosophical Transactions of Royal Society of London* **A203**, 1–42. On the propagation tremors at the surface of an elastic solid.
2. J. D. Achenbach 1980 *Wave Propagation in Elastic Solids*. Amsterdam: North-Holland Publishing Company.
3. K. Aki and P. G. Richards 1980 *Quantitative Seismology—Theory and Methods*. Vols. 1 and 2, New York: W. H. Freeman and Company.
4. A. Ben-Menahem and S. J. Singh 1981 *Seismic Waves and Sources*. New York: Springer-Verlag.
5. Y. C. Fung 1965 *Foundations of Solid Mechanics*. Englewood Cliffs, NJ: Prentice-Hall Inc.

6. M. Bouchon and K. Aki 1977 *Bulletin of the Seismological Society of America* **67**, 259–277. Discrete wavenumber representation of seismic-source wave fields.
7. M. Bouchon 1979 *Journal of Geophysical Research* **84**, 3609–3614. Discrete wavenumber representation of elastic wave fields in three-dimensional space.
8. M. Bouchon 1981 *Bulletin of the Seismological Society of America* **71**, 959–971. A simple method to calculate Green's functions for elastic layered media.
9. G. Deodatis, M. Shinozuka and A. Papageorgiou 1990a. *Journal of Engineering Mechanics* **116**, 2363–2379. Stochastic wave representation of seismic ground motion. I: F–K spectra.
10. G. Deodatis, M. Shinozuka and A. Papageorgiou 1990b *Journal of Engineering Mechanics* **116**, 2381–2399. Stochastic wave representation of seismic ground motion. II: simulation.
11. J. E. Luco and H. L. Wong 1987 *Earthquake Engineering and Structural Dynamics* **15**, 233–247. Seismic response of foundations embedded in a layered half-space.
12. R. Zhang 1994 *Journal of Sound and Vibration* **176**, 69–92. Stochastic seismic ground motion modeling with imperfectly stratified earth medium.
13. A. S. Alekseev and B. G. Mikhailenko 1980 *Journal of Geophysics* **48**, 167–172. The solution of dynamic problems of elastic wave propagation in inhomogeneous media by a combination of partial separation of variables and finite-difference methods.
14. R. J. Apsel and J. E. Luco 1983 *Bulletin of the Seismological Society of America* **73**, 931–951. On the Green's function for a layered II.
15. B. L. N. Kennet 1983. *Seismic Wave Propagation in Stratified Media*. Cambridge: Cambridge University Press.
16. M. Korn 1987 *Geophysical Journal of the Royal Astronomical Society* **88**, 345–377. Computation of wavefields in vertically inhomogeneous media by a frequency domain finite-difference method and application to wave propagation in earth models with random velocity and density perturbations.
17. J. E. Luco and R. J. Apsel 1983 *Bulletin of the Seismological Society of America* **73**, 909–929. On the Green's function for a layered half-space. Part I.
18. A. H. Olson, J. A. Orcutt and G. A. Frazier 1984. *Geophysical Journal of the Royal Astronomical Society* **77**, 421–460. The discrete wavenumber/finite element method for synthetic seismograms.
19. R. Zhang, Y. Yong and Y. K. Lin 1991a. *Journal of Engineering Mechanics* **117**, 2114–2132. Earthquake ground motion deterministic point source.
20. R. Zhang, Y. Yong and Y. K. Lin 1991b. *Journal of Engineering Mechanics* **117**, 2133–2148. Earthquake ground motion stochastic line source.
21. M. Shinozuka and G. Deodatis 1991 *Applied Mechanics Reviews* ASME **44**, 191–204. Simulation of stochastic processes by spectral representation.
22. M. Shinozuka and G. Deodatis 1996 *Applied Mechanics Reviews* ASME **49**, 1–53. Simulation of multi-dimensional Gaussian stochastic fields by spectral representation.
23. Y. Yong, R. Zhang and J. Yu 1997a. *International Journal of Soil Dynamics and Earthquake Engineering* **16**, 295–306. Motion of foundation on a layered soil medium—I. Impedance characteristics.
24. Y. Yong, R. Zhang and J. Yu 1997b. *International Journal of Soil Dynamics and Earthquake Engineering* **16**, 307–316. Motion of foundation on a layered soil medium—II. Response analysis.
25. J. W. Dunkin 1965 *Bulletin of the Seismological Society of America* **55**, 335–358. Computation of modal solutions in layered, elastic media at high frequencies.
26. B. L. N. Kennet 1973 *Geophysical Journal of the Royal Astronomical Society* **28**, 249–266. Seismic waves scattering by obstacles on interfaces.
27. B. Chouet 1987 *Bulletin of the Seismological Society of America* **77**, 14–27. Representation of an extended seismic source in a propagator-based formalism.
28. R. J. Archuleta and S. Hartzell 1981 *Bulletin of the Seismological Society of America* **71**, 939–957. Effects of fault finiteness on near-source ground motion.

29. R. ZHANG and G. DEODATIS 1996 *Earthquake Engineering and Structural Dynamics* **25**, 465–481. Seismic ground motion synthetics of the 1989 Loma Prieta earthquake.
30. Y. K. LIN 1963 *Journal of Applied Mechanics* **30**, 555–558. Applications of nonstationary shot noise in the study of system response to a class of nonstationary excitations.
31. C. A. CORNELL 1964 *Standford Univ., Civil Eng. Dept., Report*. 34. Stochastic process models in structural engineering.
32. K. AKI and K. L. LARNER 1970 *Journal of Geophysical Research* **75**, 933–954. Surface motion of a layered medium having an irregular interface due to incident plane SH wave.
33. B. L. N. KENNETT 1972 *Geophysical Journal of the Royal Astronomical Society* **27**, 301–325. Seismic waves in laterally inhomogeneous media.
34. Y. K LIN 1986 *Journal of Probabilistic Engineering Mechanics* **1**, 219–223. On random pulse train and its evolutionary spectral representation.
35. Y. YONG and Y. K. LIN 1989 *Journal of Sound and Vibration* **129**, 99–118. Propagation of decaying waves in periodic and piecewise periodic structures of finite length.
36. R. ZHANG and M. SHINOZUKA 1996 *Journal of Sound and Vibration* **195**, 1–16. Effects of irregular boundaries in layered half-space on seismic waves.
37. R. ZHANG, L. ZHANG and M. SHINOZUKA 1997a *Journal of Applied Mechanics* **64**, 50–58. Seismic waves in a laterally inhomogeneous layered medium. I: theory.
38. R. ZHANG, L. ZHANG and M. SHINOZUKA 1997b *Journal of Applied Mechanics* **64**, 59–65. Seismic waves in a laterally inhomogeneous layered medium. II: analysis.

APPENDIX A: IMPORTANT MATRICES

For P-SV wave motion,

$$M_{u,d}(i) = \begin{bmatrix} \mp \mathrm{i} q_{Pi} \varepsilon_{Pi} & \kappa_r \varepsilon_{Si}/\omega \\ \kappa_r \varepsilon_{Pi}/\omega & \mp \mathrm{i} q_{Si} \varepsilon_{Si} \end{bmatrix}, \tag{A1}$$

$$N_{u,d}(i) = \begin{bmatrix} \rho_i (2v_{Si}^2 \kappa_r^2/\omega^2 - 1)\varepsilon_{Pi} & \mp 2\mathrm{i}\rho_i v_{Si} \kappa_r q_{Si} \varepsilon_{Si}/\omega \\ \mp 2\mathrm{i}\rho_i v_{Si} \kappa_r q_{Pi} \varepsilon_{Pi}/\omega & \rho_i (2v_{Si}^2 \kappa_r^2/\omega^2 - 1)\varepsilon_{Si} \end{bmatrix} \tag{A2}$$

and for SH wave motion,

$$M_{u,d}(i) = \varepsilon_{Si}/v_{Si}, \quad N_{u,d}(i) = \mp \mathrm{i}\rho_i v_{Si} q_{Si} \varepsilon_{Si}, \tag{A3}$$

where v_{Pi} and v_{Si} and ρ_i are, respectively, the P and S wave speeds and density in the ith layer, and

$$q_{Pi} = \sqrt{1/v_{Pi}^2 - \kappa_r^2/\omega^2}, \qquad q_{Si} = \sqrt{1/v_{Si}^2 - \kappa_r^2/\omega^2}, \tag{A4}$$

$$\varepsilon_{Pi} = (2\rho q_{Pi})^{-1/2}, \qquad \varepsilon_{Si} = (2\rho q_{Si})^{-1/2}. \tag{A5}$$

To account for damping, real-valued speed v_{Pi} and v_{Si} can be replaced by a pair of complex ones, i.e., by $v_{Pi}[1 + \mathrm{i}\,\mathrm{sgn}(\omega)/(2Q_{Pi})]$ and $v_{Si}[1 + \mathrm{i}\,\mathrm{sgn}(\omega)/(2Q_{Si})]$, where $\mathrm{sgn}(\omega)$ denotes the sign of frequency ω, Q_{Pi} and Q_{Si} are the attenuation factors for

P and S waves in layer i. The branch cuts for the radicals in the expression for q_{Pi} and q_{Si} are taken to be

$$\mathrm{Im}(\omega q_{Pi}) \geqslant 0, \qquad \mathrm{Im}(\omega q_{Si}) \geqslant 0. \tag{A6}$$

The reflection and transmission matrices in layer i, which is bounded by depths z_{i-1}^{+} and z_i^{-}, are

$$R(z_{i-1}^{+}, z_i^{-}) = R(z_i^{-}, z_{i-1}^{+}) = 0, \tag{A7}$$

$$T(z_{i-1}^{+}, z_i^{-}) = T(z_i^{-}, z_{i-1}^{+}) = \begin{cases} \mathrm{diag}[e^{i\omega q_{Pi}\Delta z}\, e^{i\omega q_{Si}\Delta z}] & (P-SV), \\ e^{i\omega q_{Si}\Delta z} & (SH), \end{cases} \tag{A8}$$

where diag indicates a diagonal matrix and $\Delta z = |z_i^{-} - z_{i-1}^{+}|$. The reflection and transmission matrices at the interface with depth z_i bounded by z_i^{-} and z_i^{+} are

$$R(z_i^{-}, z_i^{+}) = Q_{12} Q_{22}^{-1}, \; R(z_i^{+}, z_i^{-}) = -Q_{22}^{-1} Q_{21}, \tag{A9}$$

$$T(z_i^{-}, z_i^{+}) = Q_{22}^{-1}, \; T(z_i^{+}, z_i^{-}) = Q_{11} - Q_{12} Q_{22}^{-1} Q_{21}, \tag{A10}$$

where

$$Q_{11} = -iN_d^{\mathrm{T}}(i) M_u(i+1) + iM_d^{\mathrm{T}}(i) N_u(i+1), \tag{A11}$$

$$Q_{12} = -iN_d^{\mathrm{T}}(i) M_d(i+1) + iM_d^{\mathrm{T}}(i) N_d(i+1), \tag{A12}$$

$$Q_{21} = -iN_u^{\mathrm{T}}(i) M_u(i+1) - iM_u^{\mathrm{T}}(i) N_u(i+1), \tag{A13}$$

$$Q_{22} = -iN_u^{\mathrm{T}}(i) M_d(i+1) - iM_u^{\mathrm{T}}(i) N_d(i+1). \tag{A14}$$

The reflection matrix at the free surface is

$$R(0^{+}, 0) = -[N_d(1)]^{-1} N_u(1). \tag{A15}$$

Based on the fundamental reflection and transmission matrices for each uniform layer, each interface between each pair of neighboring layers and the ground surface (equations (A7)–(A15)), the corresponding reflection and transmission matrices between any two depths can be constructed using the composite rule [15, 22]

$$R(z_i, z_k) = R(z_i, z_j) + T(z_j, z_i) R(z_j, z_k) [I - R(z_j, z_i) R(z_j, z_k)]^{-1} T(z_i, z_j), \tag{A16}$$

$$T(z_i, z_k) = T(z_j, z_k) [I - R(z_j, z_i) R(z_j, z_k)]^{-1} T(z_i, z_j). \tag{A17}$$

APPENDIX B: COMPUTER CODES

The following two computer codes have been developed and used to verify the observations presented in this study.

SEISMO was developed primarily by G. Deodatis, A. Papageorgiou, M. Shinozuka, and R. Zhang at Princeton University and University of Southern California over the past 10 years. It uses the discrete wavenumber technique to simulate ground motion as a result of wave propagation generated by rupturing shear-slip over a broken fault area and scattered in a half-space with laterally heterogeneous 3-D layers. The methodology is developed on the basis of the work of references [1, 3, 7, 25, 26, 27]. Its validity and accuracy were verified by comparing the numerical results using SEISMO with corresponding results obtained by reference [28]. Using seismologically consistent source models in a layered half-space, SEISMO code has successfully synthesized both near and farfield motion in the 1968 Tokachi-Oki and the 1989 Loma Prieta earthquakes (e.g., reference [29]). The magnitude (intensity), wave form (frequency content) and time duration of the synthesized Loma Prieta earthquake ground motion have been found to be consistent with the actual records.

STOQUK was developed for modelling of earthquake ground motion and simulation by Y. K. Lin, Y. Yong and R. Zhang in Florida in 1985–1991 and continue to be modified by Zhang at Princeton University in 1992–1995 and at University of Southern California in 1995–1997. The model established in STOQUK is capable of capturing both the geophysical and stochastic features of earthquakes. The methodology is based on references [11, 14–17, 30–35]. The earth is modelled as a layered half-space with irregular topography and sub-surfaces. The influence of sub-surface irregularity on ground motion, and thus structures, can be estimated both qualitatively and quantitatively. The wave motion representations can be set within the framework of either Cartisian or Cylindrical co-ordinates. The validity and accuracy of STOQUK results were verified by comparing with theoretical predictions and with corresponding results obtained by references [9, 10] and SEISMO.